Investigating the interaction between rocking amplitude and ground motion characteristics via artificial neural networks

A.I. Giouvanidis
Department of Civil and Environmental Engineering, University of Auckland, Auckland, New Zealand.

S. Karimzadeh
Department of Civil Engineering, University of Minho, ISISE, ARISE, 4800-058 Guimarães, Portugal.

S.A. Banimahd
Department of Civil Engineering, Faculty of Engineering, Ardakan University, Ardakan, Iran.

P.B. Lourenço
Department of Civil Engineering, University of Minho, ISISE, ARISE, 4800-058 Guimarães, Portugal.

ABSTRACT
This paper applies machine learning algorithms to investigate the interrelationship between seismic signal and rocking demand. Specifically, it employs Artificial Neural Networks (ANN) to predict the rocking amplitude and reveal the input variables that contribute the most to the prediction. The paper adopts a variety of rocking blocks of different sizes and slenderness, and it employs a suite of recorded earthquakes. The analysis assumes that no sliding and bouncing occur during rocking. Furthermore, solely the cases where the blocks safely return to their initial rest position after the end of the ground shaking are considered. An ANN model is trained to predict the response amplitude and identify the most critical input variables that govern safe rocking. The results unveil that the rocking amplitude is governed by a combined consideration of duration, frequency, and intensity characteristics of the ground motion. Importantly, a novel intensity measure, i.e., maximum incremental velocity, shows a substantial correlation with the rocking amplitude. Finally, the coefficient of restitution, which controls the energy dissipation of a rigid block during rocking, is found to be less influential to the peak safe rocking response compared to the remaining input variables of the rocking problem.

1 INTRODUCTION

Rocking is considered an unconventional seismic isolation paradigm as it activates the structural rotational inertia to provide seismic stability (Housner 1963). Therefore, it finds application to a variety of structural configurations (Vlachakis et al., 2021, Vlachakis et al., 2023, Bachmann et al., 2017, Dimitrakopoulos and

Giouvanidis, 2015, Giouvanidis and Dimitrakopoulos, 2017a, Giouvanidis and Dong, 2020, Manzo and Vassiliou, 2022, Manzo et al., 2022). However, rocking motion has been shown to be highly nonlinear (Giouvanidis et al., 2022) and nonsmooth (Giouvanidis and Dimitrakopoulos, 2017b). Specifically, a rocking structure is particularly sensitive to different characteristics of the ground excitation. Psycharis et al. (2013) showed the important contribution of the peak ground velocity (*PGV*) to rocking response, while Dimitrakopoulos and Paraskeva (2015) highlighted the contribution of *PGV* and a combination of the peak ground acceleration (*PGA*) with a frequency characteristic (*PGA*/*PGV*) to rocking amplitude. Later, Lachanas et al. (2023) verified the importance of *PGV* and *PGA* to the overturning mode of slender and stocky rocking structures, respectively. Further corroboration of velocity and frequency characteristics as optimal intensity measures (IMs) came from Pappas et al. (2017), Kavvadias et al. (2017), and Sieber et al. (2023). Recently, Giouvanidis and Dimitrakopoulos (2018) revealed the remarkable contribution of duration characteristics, i.e., the uniform duration t_{uni} and cumulative absolute velocity of exceedance CAV_{exc}, to the rocking amplitude.

A limitation of the above studies is the consideration of either scalar or bivariate IMs, which might not be enough to efficiently represent the impact of a seismic signal on the structural demand. Machine learning (ML) methodologies can potentially aid in revealing the underlying nonlinearity of such interaction (Banimahd et al., 2024, Mohammadi et al., 2023a, Mohammadi et al., 2023b, Karimzadeh et al., 2023, Mignan and Broccardo, 2020). Thus, the main objective of this work is twofold: (i) to explore the ability of artificial neural network (ANN) models to predict the peak safe rocking response and (ii) to identify the critical ground motion characteristics that govern the rocking amplitude.

2 ROCKING DYNAMICS, INTENSITY MEASURES, AND ENGINEERING DEMAND PARAMETERS

The rocking block of Figure 1 is a structural model that can describe the dynamics of a wide class of rocking configurations (DeJong and Dimitrakopoulos, 2014). Under a horizontal ground excitation, the block commences rocking once the ground acceleration exceeds the minimum threshold:

$$|\ddot{u}_g| = g tan\alpha \tag{1}$$

where g is the gravitational acceleration, and α is the slenderness angle (Figure 1). During rocking, the equation that describes the rocking motion of the block is:

$$\ddot{\theta} = -p^2 \left[sin(\alpha sgn(\theta) - \theta) + \frac{\ddot{u}_g}{g} cos(\alpha sgn(\theta) - \theta) \right] \tag{2}$$

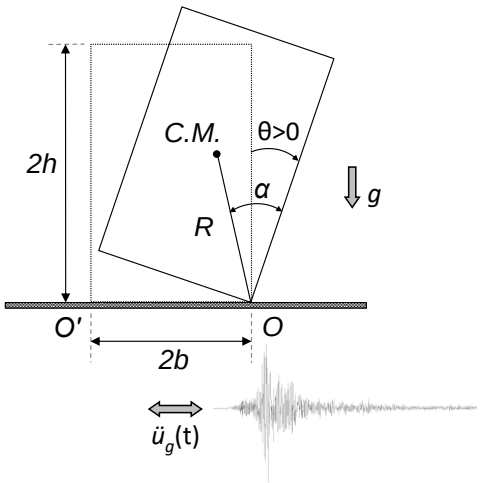

Figure 1 The rocking block model when subjected to a horizontal ground excitation.

where $p = \sqrt{3g/4R}$ is the frequency parameter of the block, and R is the half-diagonal distance. When, during rocking, the block impacts the ground, energy is lost. The amount of energy loss at impact is captured by the coefficient of restitution η and expressed as a relationship between the post- with the pre-impact angular velocities $\dot{\theta}^+ = \eta\dot{\theta}^-$ (Housner 1963). This study considers η as an independent input variable whose contribution to rocking response is investigated.

To capture the effect of ground shaking on the rocking response, this work adopts a selection of dimensionless IMs that can efficiently represent different aspects of a seismic waveform, such as frequency, amplitude, duration, and energy content. It also introduces two novel IMs, the intensity-based $pMIV/gtan\alpha$ and the frequency-based $1/\left(p\sqrt{t_{uni}/v_0}\right)$ (Banimahd et al., 2024), which, respectively, represent the amplitude and the frequency of appearance of the individual impulses formed between the accelerogram and the rocking initiation threshold.

Finally, as an engineering demand parameter, the ratio of the absolute peak rocking rotation $|\theta|_{max}$ over the slenderness angle α is chosen.

Table 1. Dimensionless intensity measures (Banimahd et al., 2024).

Category	**Intensity measure**	**Definition**
Intensity-based	$PGA/gtan\alpha$	$PGA = \max(\lvert\ddot{u}_g(t)\rvert)$ = peak ground acceleration
	$pPGV/gtan\alpha$	$PGV = \max(\lvert\dot{u}_g(t)\rvert)$ = peak ground velocity
	$pMIV/gtan\alpha$	MIV = maximum incremental velocity
Frequency-based	$PGA/pPGV$	
	$PGV/pPGD$	
	pT_m	$T_m = \sum_i(C_i^2/f_i)/\sum_i C_i^2$ = mean period
	$1/\left(p\sqrt{t_{uni}/v_0}\right)$	v_0 = number of crossings per unit of (bracketed) time
Duration-based	pt_{sig}	t_{sig} = significant duration
	pt_{uni}	t_{uni} = uniform duration
	pt_{brc}	t_{brc} = bracketed duration
	pt_{sust}	t_{sust} = sustained duration
Energy-based	$A_{RMS}/gtan\alpha$	$A_{RMS} = \sqrt{\frac{1}{t_{tot}}\int_0^{t_{tot}}(\ddot{u}_g(t))^2 dt}$ = root mean square acceleration
	$pI_A/gtan\alpha$	I_A = Arias intensity

3 THE INTERRELATIONSHIP BETWEEN SEISMIC SIGNAL AND ROCKING AMPLITUDE

To investigate the interrelationship between seismic signal and rocking amplitude, this work employs Artificial Neural Networks (ANN). Prior to training, this study conducts nonlinear dynamic analyses, the results of which serve as the input dataset for the training of the ANN model. To this end, a variety of rocking blocks are adopted with frequency parameter $0.7 \leq p \leq 4$ rad/s and slenderness angle $0.07 \leq \alpha \leq 0.4$ rad, covering a wide range of rocking configurations, e.g., building/lab contents, masonry façades, and/or bridge columns. Furthermore, the coefficient of restitution η is considered an independent input variable with values $0.72 \leq \eta \leq 0.99$ (Sorrentino et al., 2011, Galvez et al., 2022). Finally, recorded earthquakes from the PEER database (Ancheta et al., 2014) are employed to shake the rocking blocks. In total, 59,640 response-history analyses are conducted, resulting in 2,710 safe rocking cases.

In general, an ANN model consists of (at least) three layers: (i) input layer, (ii) output layer, and (iii) hidden layer(s). The appropriate number of hidden layers varies based on the complexity of the problem. Each layer consists of neurons, which are connected and interact with each other via adjustable weights. The number of neurons in the input and output layers corresponds to the number of input and output variables, respectively. On the other hand, the number hidden layers and neurons in each hidden layer varies and depends on the complexity of the problem (Haykin 2004). In this study, a single hidden layer is adequate to train the ANN model efficiently, while the hidden layer with 13 neurons provides the optimal solution (Banimahd et al., 2024). The input layer consists of 14 neurons (i.e. one for each input variable of Table 1 and the coefficient of restitution). For a more generalised ANN model, i.e., adequately robust to an unseen (new) dataset, this work divides the whole input dataset into three parts: (i) train, (ii) validation, and (iii) test dataset. The train dataset is utilised to optimise the parameters of the ANN model (i.e. weights and biases). The validation dataset is used during the training process to evaluate the performance of the trained model. The test dataset is utilised to evaluate the predictive ability of the trained ANN model. Also, to improve the stability of the model, the k-fold cross-validation approach is employed (Hastie et al., 2009). The k-fold cross-validation approach commences, assuming that 20 % of the whole dataset serves as the test dataset. This part does not participate in the learning process. The remaining 80 % is randomly divided into k groups such that k-1 subsets are used for training and the remaining one for validation. In this study, k is equal to ten (Hastie et al., 2009). Finally, the performance of the ANN model is evaluated with the test dataset via the use of different statistical metrics, such as the Pearson correlation coefficient (r_P) and the coefficient of determination (R^2).

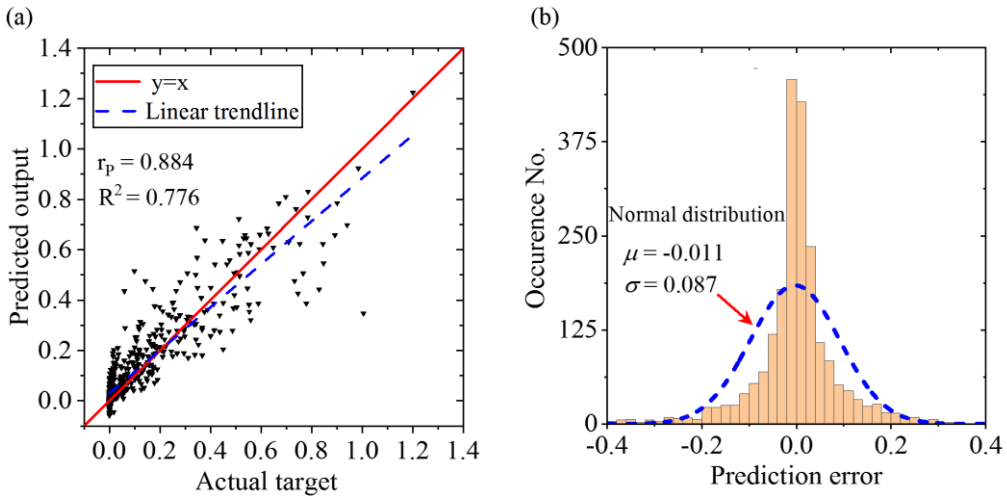

Figure 2. (a) Actual targets versus predicted outputs, and (b) distribution of the prediction error.

Figure 2a illustrates the predictive ability of the trained ANN model by plotting the actual targets with respect to the corresponding predicted outputs. In addition, Figure 2a presents the linear trendline and emphasises the difference between the ANN prediction (dashed blue line) and the perfect one (solid red line). The performance of the ANN is quantified by a Pearson correlation coefficient as high as $r_P = 0.884$ and a coefficient of determination $R^2 = 0.776$, illustrating an adequately accurate prediction of the peak safe rocking response considering that both targets and outputs are given on a natural scale where a certain level of scatter is expected−contrary to a logarithmic scale. In the same context, Figure 2b shows that the mean value of the prediction error is close to zero ($\mu = -0.011$) with a standard deviation of $\sigma = 0.087$, which confirms that the model is unbiased and the errors are random, indicating that the ANN model is a reliable predictor of the rocking amplitude.

To reveal the contribution of each input variable (i.e. the IMs of Table 1 and the coefficient of restitution η) to the rocking amplitude, this section adopts two different methodologies: (i) the Garson (Garson 1991) and (ii) the Olden (Olden and Jackson, 2002) methods. According to the Garson method, each connection weight between the hidden and output layers is partitioned into components associated with each input neuron. A limitation of the Garson method is that it solely uses the magnitude of the connection weights to calculate the importance factor. On the contrary, the Olden method considers both the magnitude and the direction (i.e. positive or negative) of the connection weights to calculate the importance factor of each input parameter to the output.

Figure 3 plots all the input variables of Table 1 and the coefficient of restitution η based on their contribution to the peak safe rocking response (from the highest to the lowest). As expected, the two methods provide slightly different results. Nevertheless, Figure 3 reveals an adequate level of consistency in the results regardless of the method used. Specifically, Figure 3 unveils that the peak safe rocking response is governed by a combination of the frequency-based pT_m, the duration-based pt_{uni}, and the intensity-based $pMIV/(gtan\alpha)$ as well as $pPGV/(gtan\alpha)$, highlighting the consistent significance of a novel IM for the rocking literature, i.e. the intensity-based $pMIV/(gtan\alpha)$. The considerable influence of the frequency of appearance of the individual impulses of exceedance $1/(p\sqrt{t_{uni}/v_0})$ and the intensity-based $PGA/(gtan\alpha)$. to the rocking amplitude is also observable. On the contrary, the contribution of the coefficient of restitution η on the peak safe rocking response is not high enough to be considered as important/dominant. Finally, note that the Olden method (Figure 3b) also reveals the sign of contribution, implying that when all input variables are considered, e.g. increase of the frequency-based $PGV/pPGD$ leads to decrease of the peak safe rocking response.

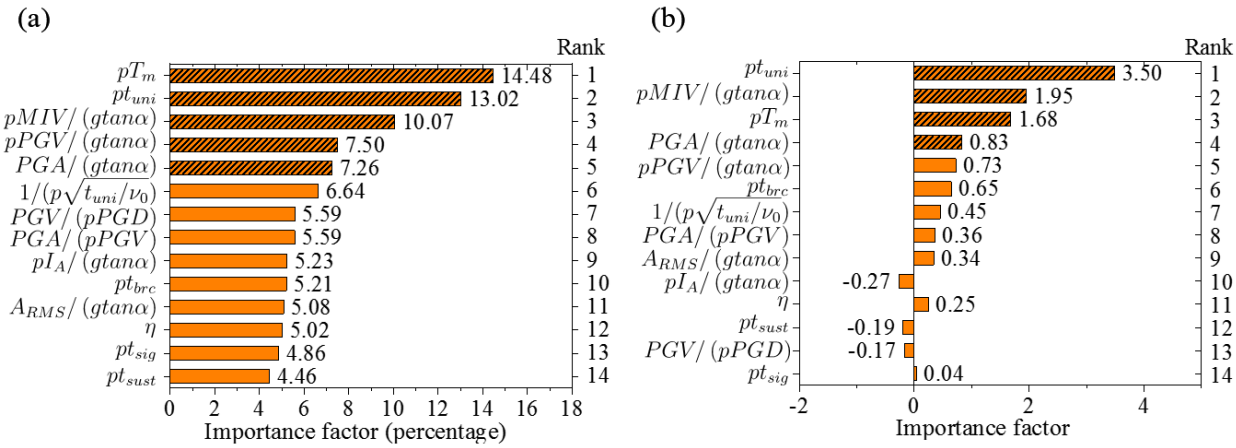

Figure 3. Significant predictors (from the most to the least important) of the peak safe rocking response based on the (a) Garson, (b) Olden methods.

4 CONCLUSIONS

This paper investigates the ability of Artificial Neural Networks (ANN) to predict the peak response of multiple rigid rocking blocks when subjected to random recorded earthquakes. The focus of this research is on cases where the rocking blocks safely return to their initial rest position after the end of the ground shaking. Thus, the main objective of this research is first (i) to train an ANN model to accurately predict the (safe) rocking amplitude and (ii) to reveal the most influential input variables on the prediction. The results unveil that a combined consideration of duration, frequency, and intensity characteristics of the ground motion shows a substantial contribution to the rocking amplitude. Interestingly, this paper also identifies a novel ground motion characteristic that shows an adequate correlation with the response, i.e., the maximum incremental velocity, while also paying special attention to the role of the coefficient of restitution, which is found to be less significant compared to the remaining input variables of the rocking problem.

ACKNOWLEDGEMENTS

This study has been partly funded by the STAND4HERITAGE project (new STANDards FOR seismic assessment of built cultural HERITAGE) that has received funding from the European Research Council (ERC) under the European Union's Horizon 2020 research and innovation program (Grant No. 833123) as an Advanced Grant. This work was also partly financed by FCT/MCTES through national funds (PIDDAC) under the R&D Unit Institute for Sustainability and Innovation in Structural Engineering (ISISE), under reference UIDB/04029/2020, and under the Associate Laboratory Advanced Production and Intelligent Systems ARISE under reference LA/P/0112/2020. The opinions and conclusions presented in this paper are those of the authors and do not necessarily reflect the views of the sponsoring organisations.

REFERENCES

Ancheta TD, Darragh RB, Stewart JP, Seyhan E, Silva WJ, Chiou BSJ, Wooddell KE, Graves RW, Kottke AR, Boore DM, Kishida T, Donahue JL (2014). "NGA-West2 database". *Earthquake Spectra*, **30**(3):989-1005. https://doi.org/10.1193/070913EQS197M

Bachmann JA, Vassiliou MF, Stojadinović B (2017). "Dynamics of rocking podium structures". *Earthquake Engineering & Structural Dynamics*, **46**(14):2499-2517. https://doi.org/10.1002/eqe.2915

Banimahd SA, Giouvanidis AI, Karimzadeh S, Lourenço PB (2024). "A multi-level approach to predict the seismic response of rigid rocking structures using artificial neural networks". *Earthquake Engineering & Structural Dynamics*. https://doi.org/10.1002/eqe.4110

DeJong MJ, Dimitrakopoulos EG (2014). "Dynamically equivalent rocking structures". *Earthquake Engineering & Structural Dynamics*, **43**(10):1543-1563. https://doi.org/10.1002/eqe.2410

Dimitrakopoulos EG, Giouvanidis AI (2015). "Seismic response analysis of the planar rocking frame". *Journal of Engineering Mechanics*, **141**(7):04015003. https://doi.org/10.1061/(ASCE)EM.1943-7889.0000939

Dimitrakopoulos EG, Paraskeva TS (2015). "Dimensionless fragility curves for rocking response to near-fault excitations". *Earthquake Engineering & Structural Dynamics*, **44**(12):2015-2033. https://doi.org/10.1002/eqe.2571

Galvez F, Sorrentino L, Dizhur D, Ingham JM (2022). "Seismic rocking simulation of unreinforced masonry parapets and façades using the discrete element method". *Earthquake Engineering & Structural Dynamics*, **51**(8):1840-1856. https://doi.org/10.1002/eqe.3641

Garson DG (1991). "Interpreting neural network connection weights". *Artificial Intelligence Expert*, **6**:47-51. https://dl.acm.org/doi/10.5555/129449.129452

Giouvanidis AI, Dimitrakopoulos EG (2017a). "Seismic performance of rocking frames with flag-shaped hysteretic behavior". *Journal of Engineering Mechanics*, **143**(5):04017008. https://doi.org/10.1061/(ASCE)EM.1943-7889.0001206

Giouvanidis AI, Dimitrakopoulos EG (2017b). "Nonsmooth dynamic analysis of sticking impacts in rocking structures". *Bulletin of Earthquake Engineering*, **15**:2273-2304. https://doi.org/10.1007/s10518-016-0068-4

Giouvanidis AI, Dimitrakopoulos EG (2018). "Rocking amplification and strong-motion duration". *Earthquake Engineering & Structural Dynamics*, **47**(10):2094-2116. https://doi.org/10.1002/eqe.3058

Giouvanidis AI, Dimitrakopoulos EG, Lourenço PB (2022). "Chattering: an overlooked peculiarity of rocking motion". *Nonlinear Dynamics*, **109**(2):459-477. https://doi.org/10.1007/s11071-022-07578-1

Giouvanidis AI, Dong Y (2020). "Seismic loss and resilience assessment of single-column rocking bridges". *Bulletin of Earthquake Engineering*, **18**(9):4481-4513. https://doi.org/10.1007/s10518-020-00865-5

Hastie T, Tibshirani R, Friedman J. (2009). "*The Elements of Statistical Learning: Data Mining, Inference, and Prediction*". New York, Springer Science & Business Media. https://link.springer.com/book/10.1007/978-0-387-21606-5

Haykin S (2004). "*Kalman filtering and neural networks*". John Wiley & Sons. https://onlinelibrary.wiley.com/doi/book/10.1002/0471221546

Housner GW (1963). "The behavior of inverted pendulum structures during earthquakes". *Bulletin of the Seismological Society of America*, **53**(2):403-417. https://doi.org/10.1785/BSSA0530020403

Karimzadeh S, Mohammadi A, Hussaini SMS, Caicedo D, Askan A, Lourenço PB (2023). "ANN-based ground motion model for Turkey using stochastic simulation of earthquakes". *Geophysical Journal Int*ernational, **236**(1):413-429. https://doi.org/10.1093/gji/ggad432

Kavvadias IE, Vasiliadis LK, Elenas A (2017). "Seismic response parametric study of ancient rocking columns". *International Journal of Architectural Heritage*, **11**(6):791-804. https://doi.org/10.1080/15583058.2017.1298009

Lachanas CG, Vamvatsikos D, Dimitrakopoulos EG (2023). "Intensity measures as interfacing variables versus response proxies: The case of rigid rocking blocks". *Earthquake Engineering & Structural Dynamics*, **52**(6):1722-1739. https://doi.org/10.1002/eqe.3838

Manzo RN, Vassiliou MF (2022). "Cyclic tests of a precast restrained rocking system for sustainable and resilient seismic design of bridges". *Engineering Structures*, **252**:113620. https://doi.org/10.1016/j.engstruct.2021.113620

Manzo RN, Vassiliou MF, Mouzakis H, Badogiannis E (2022). "Shaking table tests of a resilient bridge system with precast reinforced concrete columns equipped with springs". *Earthquake Engineering & Structural Dynamics*, **51**(1):213-239. https://doi.org/10.1002/eqe.3563

Mohammadi A, Karimzadeh S, Banimahd SA, Ozsarac V, Lourenço PB (2023a). "The potential of region-specific machine-learning-based ground motion models: Application to Turkey". *Soil Dynamics & Earthquake Engineering*, **172**:108008. https://doi.org/10.1016/j.soildyn.2023.108008

Mohammadi A, Karimzadeh S, Yaghmaei-Sabegh S, Ranjbari M, Lourenço PB (2023b). "Utilising artificial neural networks for assessing seismic demands of buckling restrained braces due to pulse-like motions". *Buildings*, **13**(10):2542. https://doi.org/10.3390/buildings13102542

Olden JD, Jackson DA (2002). "Illuminating the "black box": a randomization approach for understanding variable contributions in artificial neural networks". *Ecological Modelling*, **154**(1-2):135-150. https://doi.org/10.1016/S0304-3800(02)00064-9

Pappas A, Sextos A, Da Porto F, Modena C (2017). "Efficiency of alternative intensity measures for the seismic assessment of monolithic free-standing columns". *Bulletin of Earthquake Engineering*, **15**:1635-1659. https://doi.org/10.1007/s10518-016-0035-0

Psycharis IN, Fragiadakis M, Stefanou I (2013). "Seismic reliability assessment of classical columns subjected to near-fault ground motions". *Earthquake Engineering & Structural Dynamics*, **42**(14):2061-2079. https://doi.org/10.1002/eqe.2312

Sieber M, Vassiliou MF, Anastasopoulos I (2022). "Intensity measures, fragility analysis and dimensionality reduction of rocking under far-field ground motions". *Earthquake Engineering & Structural Dynamics*, **51**(15):3639-3657. https://doi.org/10.1002/eqe.3740

Sorrentino L, AlShawa O, Decanini LD (2011). "The relevance of energy damping in unreinforced masonry rocking mechanisms. Experimental and analytic investigations". *Bulletin of Earthquake Engineering*, **9**:1617-1642. https://doi.org/10.1007/s10518-011-9291-1

Vlachakis G, Giouvanidis AI, Mehrotra A, Lourenço PB (2021). "Numerical block-based simulation of rocking structures using a novel universal viscous damping model". *Journal of Engineering Mechanics*, **147**(11):04021089. https://doi.org/10.1061/(ASCE)EM.1943-7889.0001985

Vlachakis G, Colombo C, Giouvanidis AI, Savalle N, Lourenço PB (2023). "Experimental characterisation of dry-joint masonry structures: Interface stiffness and interface damping". *Construction and Building Materials*, **392**:130880. https://doi.org/10.1016/j.conbuildmat.2023.130880